Aberrant expression of serine/threonine kinase Pim-3 in hepatocellular carcinoma development and its role in the proliferation of human hepatoma cell lines

Title: **Aberrant expression of serine/threonine kinase Pim-3 in hepatocellular carcinoma development and its role in the proliferation of human hepatoma cell lines**

Chifumi Fujii[1, 2], Yasunari Nakamoto[3], Peirong Lu[1], Koichi Tsuneyama[4], Boryana K. Popivanova[1], Shuichi Kaneko[3], and Naofumi Mukaida[1, 2, *]

[1]Division of Molecular Bioregulation and [2]Center for the Development of Molecular Target Drugs, Cancer Research Institute, [3]Department of Gastroenterology, Graduate School of Medical Science, Kanazawa University, 13-1 Takara-machi, Kanazawa, Ishikawa 920-0934, and [4]Department of Surgical Pathology, Toyama Medical and Pharmaceutical University Hospital, 2630 Sugitani, Toyama 930-0194, Japan

Short running title: Pim-3 in hepatocellular carcinoma

[*]Correspondence to Division of Molecular Bioregulation, Cancer Research Institute, Kanazawa University, 13-1 Takara-machi, Kanazawa, Ishikawa 920-0934, Japan.
Tel: +81-76-265-2767; Fax: +81-76-234-4520;
E-mail: naofumim@kenroku.kanazawa-u.ac.jp

Key Words: protein serine-threonine kinases, pre-malignant lesions, hepatocellular carcinoma, RNA interference, apoptosis

The abbreviations used are: BSA, bovine serum albumin; DMEM, Dulbecco's modified Eagle's medium; FBS, fetal bovine serum; FDD, fluorescent differential display; GAPDH, glyceraldehyde 3-phosphate dehydrogenase; HBV, hepatitis B virus; HCV, hepatitis C virus; HBs, HBV surface; HBsAg, HBV surface antigen; HBsTg, HBs transgenic mice; HCC, hepatocellular carcinoma; IL, interleukin; PBS (-), phosphate

buffered saline; PCR, polymerase chain reaction; RNAi, RNA interference; RT-PCR, reverse transcription-polymerase chain reaction; siRNA, short interfering RNA; STAT, signal transducers and activators of transcription; VCP, valosine containing protein.

DNA Data Bank of Japan Accession Number AB114795

Journal Category: Cancer Cell Biology

ABSTRACT

Most cases of human hepatocellular carcinoma develop after persistent chronic infection with human hepatitis B virus or hepatitis C virus, and host responses are presumed to have major roles in this process. To recapitulate this process, we have developed the mouse model of hepatocellular carcinoma using hepatitis B virus surface antigen transgenic mice. In order to identify the genes associated with hepatocarcinogenesis in this model, we compared the gene expression patterns between pre-malignant lesions surrounded by hepatocellular carcinoma tissues and control liver tissues by using a fluorescent differential display analysis. Among the genes which were expressed differentially in the pre-malignant lesions, we focused on Pim-3, a member of a proto-oncogene *Pim* family, because its contribution to hepatocarcinogenesis remains unknown. Moreover, the unavailability of the nucleotide sequence of full-length human Pim-3 cDNA prompted us to clone it from the cDNA library constructed from a human hepatoma cell line, HepG2. The obtained 2,392 bp human Pim-3 cDNA encodes a predicted open reading frame consisting of 326 amino acids. Pim-3 mRNA was selectively expressed in human hepatoma cell lines, but not in normal liver tissues. Moreover, Pim-3 protein was detected in human hepatocellular carcinoma tissues and cell lines but not in normal hepatocytes. Furthermore, cell proliferation was attenuated and apoptosis was enhanced in human hepatoma cell lines by the ablation of Pim-3 gene with RNA interference. These observations suggest that aberrantly expressed Pim-3 can cause autonomous cell proliferation and/or prevent apoptosis in hepatoma cell lines.

INTRODUCTION

Hepatocellular carcinoma (HCC) ranks the eighth cause of death among human cancers and is endemic in Asia, Africa, and southern Europe. Most cases of HCC arise from persistent chronic infection with human hepatitis B virus (HBV) or hepatitis C virus (HCV)[1]. Host responses are presumed to be involved in the development of HCC among patients harboring HBV or HCV, because these viruses lack apparent oncogenes and the infected patients develop HCC after suffering from chronic hepatitis-related pathology[2, 3].

Hepatitis virus infection induces the generation of virus antigen-specific cytotoxic T lymphocytes, which have been implicated in both the eradication of viruses and liver injury[4]. Cycles of cytotoxic T lymphocyte-mediated liver cell destruction and regeneration are thought to prepare the mitogenic environment[4, 5]. In order to elucidate the molecular and cellular mechanism of HCC initiation and development, one of us (Y. Nakamoto) has established a mouse model of HCC by using HBV surface antigen (HBsAg) transgenic mice (HBsTg)[6]. In this model, bone marrow cells and splenocytes were obtained from syngeneic wild-type mice, which were immunized with HBsAg and were transplanted into HBsTg mice, which were myeloablated beforehand. At 15 months after the transplantation, the transgenic mice developed multiple foci of HCC surrounded by non-malignant areas consisting of hepatocytes with atypical nuclear configuration[6, 7].

To obtain the molecular insights on hepatocarcinogenesis, we compared the gene expression pattern between non-tumor portion of this model as a pre-malignant lesion and normal tissues by using a fluorescent differential display (FDD) analysis. We observed that several genes are expressed differentially in this pre-malignant lesion, compared with normal liver tissues. Of interest is that the gene expression of Pim-3, originally identified as depolarization-induced gene in a rat pheochromocytoma cell line[8], was enhanced in this pre-malignant lesion. Here, we demonstrated that Pim-3

was expressed aberrantly in human HCC tissues and hepatoma cell lines but not normal liver tissues. We also provided evidence to suggest the involvement of Pim-3 in the proliferation of human hepatoma cell lines.

MATERIALS AND MATHODS

Experimental animals

HBsAg transgenic mouse lineage 107-5D (official designation Tg[Alb-1,HBV]Bri66; inbred B10D2, H-2^d) was provided by Dr. F. V. Chisari (The Scripps Research Institute, La Jolla, CA)[9]. Lineage 107-5D contains the entire HBV envelope-coding region (subtype ayw) under the transcriptional control of the mouse albumin promoter, and expresses the HBV small, middle, and large envelope proteins in their hepatocytes[9]. They display no evidence of liver disease during their lifetime unless they receive the adoptive transfer of HBsAg-specific cytotoxic T lymphocytes[9], due to their immunological tolerance to the HBs transgene at the T cell level[10].

Chronic hepatitis-related liver disease model was generated as described previously[6]. Briefly, after male HBsAg transgenic mice were thymectomized and irradiated (900 cGy), their hematopoietic system was reconstituted with the bone marrow cells from syngeneic non-transgenic B10D2 (H-2^d) mice. At 1 week after the bone marrow transplantation, the animals received 10^8 splenocytes from syngeneic non-transgenic B10D2 (H-2^d) mice that were infected intraperitoneally with a recombinant vaccinia virus expressing HBsAg 3 wk before the splenocyte transfer. At 12 to 15 months after the lymphocyte transfer, multiple HCC foci developed in mice[6, 7]. Non-tumor and tumor portions were demarcated macroscopically and were removed separately. A pathologist without a prior knowledge on the experimental procedures confirmed the presence of hepatocytes with atypical configurations but not malignant cells in this non-tumor potion. Hence, non-tumor portions were designated as pre-malignant lesions in the following experiments. Liver tissues were also obtained from untreated or HBsTg mice transplanted with tolerant splenocytes as a control.

Fluorescent differential display

Total RNAs extracted from liver tissues were subjected to FDD according to the method described by Ito and colleagues[11]. Briefly, total RNAs were isolated with

RNA-Bee (Biotecx Laboratories, Inc.), followed by the treatment with RNase-free DNase (Takara Shuzo, Kyoto, Japan). The purified total RNAs (2.5 μg) were reverse-transcribed with SuperScript II reverse transcriptase (Invitrogen) and fluorescein-labeled anchor primer, $GT_{15}A$, $GT_{15}C$, or $GT_{15}G$. The resultant cDNA equivalent to 50 ng of RNA was subjected to polymerase chain reaction (PCR) with 0.5 μM anchor primer, 0.5 μM arbitrary primer (10 mer kit A; Operon), 50 μM each dNTP, 1 unit of *Gene Taq* DNA polymerase (Nippon Gene, Toyama, Japan), and 1 unit of *Taq* DNA polymerase (Takara Shuzo). PCR products were separated with 6% polyacrylamide-8 M urea gel and analyzed by employing Vistra Fluor Imager SI (Molecular Dynamics). The bands of interest were excised from the gel and cloned into pSTBlue-1 Vector (Novagen). The inserted cDNA was sequenced with CEQ 2000 DNA Analysis System (Beckman Coulter) and analyzed with the BLAST program to search the GeneBank database.

Cell culture

Human hepatoma cell lines (HepG2, Hep3B, HLE, HLF, HuH7, and SK-Hep1) were maintained in Dulbecco's modified Eagle's medium (DMEM; Sigma) supplemented with 10% heat-inactivated fetal bovine serum (FBS; Atlanta Biologicals, Norcross, Ga.) at 37 ^{o}C in a humidified atmosphere with 5% CO_2 in the air[12].

Semi-quantitative reverse transcription-polymerase chain reaction (RT-PCR)

Total RNAs were isolated with RNA-Bee (Biotecx Laboratories, Inc.), followed by the treatment with RNase-free DNase (Takara Shuzo, Kyoto, Japan), and a semi-quantitative RT-PCR analysis was performed as described previously[13]. The cDNA was amplified using the sets of the primers that specifically amplify *Pim* family kinases and glyceraldehyde 3-phosphate dehydrogenase (GAPDH). The sequences are as follows; Pim-1, sense 5'-CCCGAGCTATTGAAGTCTGA-3', antisense 5'-CTGTGCAGATGGATCTCAGA-3'; Pim-2, sense 5'-CATCCCCAGCAGCTCTTTAG-3', antisense 5'-CAGTAGGGTCCCTCACCAAA-3'; Pim-3, sense

5’-AAGCAGTGACCTCTGACCCCTGGTGACC-3’, antisense 5’-CAGCGGAACCGCTCATTGCCAATGG-3’; GAPDH, sense 5’-ACCACAGTCCATGCCATCAC-3’, antisense 5’-TCCACCACCCTGTTGCTGTA-3’. The resultant PCR products were separated on 1.5% agarose gel and visualized by ethidium bromide staining. The band intensities were measured using NIH Image Analysis Software Ver 1.61 (National Institutes of Health, Bethesda, MD) and the ratios to GADPH were calculated.

cDNA library construction and screening

Total RNA was isolated from HepG2 cell line and polyA mRNA was separated by *Oligotex*^{TM}*-dT30 <Super>* mRNA Purification kit (Takara Shuzo). cDNA was synthesized with SuperScript II reverse transcriptase (Invitrogen) and oligo-dT primer, and cDNA library was constructed in pCMVSPORT6 (Invitrogen) with *Escherichia coli* DH10B (Invitrogen), according to the manufacturer’s instructions. The initial screening was performed using GENE TRAPPER® cDNA Positive Selection System (Invitrogen) and the oligomer, CTGTGAAGCACGTGGTGAAG, as a probe. The obtained colonies were subjected to colony PCR screening with the sets of primers described above. The inserted cDNA was sequenced with CEQ 2000 DNA Analysis System (Beckman Coulter).

Northern blot analysis

Human Pim-3 mRNA expression was analyzed by using Human 12-Lane MTN^{TM} Blot (Clontech, Palo Alto, CA). *In vitro* transcribed digoxigenin-labeled probes were hybridized overnight at appropriate temperatures (70 ^{o}C for Pim-3 and 68 ^{o}C for GAPDH). After being washed sequentially each for 15 min in 2 x and 0.5 x SSC buffer containing 0.1% sodium dodecyl sulfate at room temperature and at 68 ^{o}C, respectively, the hybridized probes were detected by the DIG detection kit (Boehringer Mannheim Biochemicals), according to the manufacturer’s instructions.

Preparation of anti-Pim-3 polyclonal antibodies

Anti-Pim-3 antibodies were prepared by Asahi Techno Glass Co. (Tokyo,

Japan). Briefly, two chickens were immunized with keyhole limpet hemocyanine-conjugated Pim-3 peptide, CGPGGVDHLPVKILQPAKAD, which corresponds to the amino acid residues between 13 and 32 in human Pim-3 and is conserved in murine Pim-3, and their egg yolks were harvested before and after the immunization. IgY proteins were purified with EGGstract® IgY Purification System (Promega) according to the manufacturer's instructions, and they were affinity-purified with Pim-3 peptide conjugated NHS-activated HP (Amersham Biosciences, Tokyo, Japan). Purified antibodies were quantified by measuring the absorbance at 280 nm.

Immunohistochemical analysis

Human liver specimens were surgically obtained from the patients with their informed consent, and mouse liver tissues were obtained from HBsTg mouse at the indicated time intervals after splenocyte transfer. Paraffin-embedded tissue sections were deparaffinized in xylene and rehydrated through graded concentrations of ethanol (100% - 70%). After incubation with 0.3% hydrogen peroxide in 10 mM phosphate buffer, pH 7.4, containing 150 mM NaCl (phosphate buffered saline; PBS (-)), sections were incubated sequentially with 3% normal rabbit serum (DAKO, Kyoto, Japan) and 2% bovine serum albumin (BSA) in PBS (-) and with Avidin-Biotin blocking kit (Vector Laboratories). Subsequently, the slides were treated with 10 μg/ml anti-Pim-3 IgY or pre-immunized IgY at 4 ^{o}C overnight, followed by the incubation with 2.5 μg/ml biotin-conjugated rabbit anti-chicken IgY antibodies (Promega) at room temperature for 30 min. The immune complexes were visualized by using the Vectastain Elite ABC kit (Vector Laboratories) and Vectastain DAB substrate kit (Vector Laboratories) according to the manufacturer's instructions. The slides were counterstained with hematoxylin (DAKO), mounted, and observed under a microscope (BX-50; Olympus, Tokyo, Japan).

Immunocytochemical analysis of HuH7 cells

Cells were cultured on Lab-Tec chamber slides (Nalge Nunc, Roskide, Denmark). They were fixed with 4% paraformaldehyde in PBS (-) and permeated in methanol. Then, they were blocked by incubation with 3% normal rabbit serum and

2 % BSA in PBS (-) at room temperature for 30 min, and with Avidin-Biotin blocking kit. Subsequently, they were treated with 20 μg/ml affinity-purified anti-Pim-3 IgY or pre-immunized IgY at 4 ^{o}C overnight, with 2.5 μg/ml biotin-labeled rabbit anti-chicken IgY at room temperature for 30 min. The signals were amplified and visualized by the Vectastain Elite ABC kit and Vectastain DAB substrate kit according to the manufacturer's instructions. The slides were counterstained with methylgreen (DAKO), mounted, and observed under a microscope (BX-50; Olympus).

RNA interference (RNAi)

Short interfering RNA (siRNA) was synthesized with *Silencer*^{TM} siRNA Construction Kit (Ambion) according to the manufacturer's instructions. By employing siRNA Target Finder and Design Tool (Ambion), siRNA duplexes were designed to target AA(N_{19})UU sequences in the open reading frame of mRNA encoding Pim-3. The selected siRNA target sequence (5'-GCACGUGGUGAAGGAGCGG-3' corresponding to 642-661) was further subjected to BLAST searches against other human genome sequences to ensure its target specificity. We identified two distinct cDNAs, which exhibit identity with the target sequence at 16 out of 19 nucleotides. However, we could not detect any specific bands corresponding to these cDNAs in HuH7 and Hep3B cell lines by RT-PCR analysis (our unpublished data), further indicating the specificity of the used target sequence. Scramble siRNA (5'-GCGCGCUUUGUAGGAUUCG-3' designed by B-Bridge International, inc.) was used as a negative control. Each siRNA duplex (final concentration 50 nM) was mixed with 12.5 μl and 12 μl of Lipofectamine 2000 (Invitrogen) for HuH7 and Hep3B, respectively. The mixtures were added into 2.5 ml of Opti-MEM (Invitrogen) and allowed to stand at room temperature for 20 min. The final mixture was then added directly into the semi-confluent cells in 6-cm culture dishes, which were washed with serum-free DMEM beforehand. The following day, 2.5 ml of DMEM plus 20% FBS medium was added to adjust the FBS concentration to 10%. At the indicated time intervals, cells were harvested for further analyses.

Semi-quantitative RT-PCR analysis of siRNA transfectant

Hep3B and HuH7 cells were harvested at 2 and 4 days after the transfection, respectively. Total RNAs were extracted and a semi-quantitative RT-PCR analysis was performed as described above. The cDNA was amplified using the sets of the primers that specifically amplify Pim-3 (sense 5'-ATGCTGCTCTCCAAGTTCGGCTCCCTGGCG-3', antisense 5'-TCCTGTGCCGGCTCGGGTCGCTCCAGCACC-3') and GAPDH.

Cell proliferation assay

Cells were trypsinized at 2 days after the transfection, and 5 x 10^3 cells were plated to each well of 96-well plate. This time point was designated as day 0. The cell viability was determined every day using WST-1 reagent (an MTT analog from Boehringer Mannheim Biochemicals) according to the manufacturer's instructions. The ratios to day 0 were calculated.

Cell cycle analysis by a flow cytometry

HuH7 cells were harvested at 4 days after the transfection and fixed with graded concentrations of ethanol on ice. Then, they were incubated with 50 μg/ml propidium iodide and 1 μg/ml of RNase A for 30 min at room temperature, and quenched by adding EDTA to a final concentration of 10 μM. The filtered cells were analyzed using a FACSCaliber (Becton Dickinson, Bedford, Mass.). The distribution in each cell cycle phase was determined by using Cell Quest analysis software (Becton Dickinson).

Chromatin condensation analysis by Hoechst 33258

HuH7 and Hep3B cells were harvested at 4 days after the transfection and stained with Hoechst 33258 in order to detect the cells with condensed nuclei under a fluorescence microscope (BX-50; Olympus).

RESULTS

Identification of the genes differentially expressed in pre-malignant liver tissue

We compared the gene expression patterns between pre-malignant lesions and normal liver tissues by employing a FDD method. The determination of the nucleotide sequence of the resultant bands identified 24 and 19 distinct genes among the up-regulated and down-regulated bands in pre-malignant lesions, respectively (Table 1). Among these genes, Pim-3 expression has not been reported in normal hepatocytes. Hence, we focused on Pim-3, a member of proto-oncogene *Pim* family including Pim-1 and Pim-2. A semi-quantitative RT-PCR analysis confirmed that Pim-3 mRNA expression was significantly enhanced in the pre-malignant tissues and to a lesser degree, in HCC tissues, compared with control (Fig. 1). In contrast, specific Pim-1 and Pim-2 transcripts were barely detected under these conditions (Fig. 1). These results indicate that Pim-3 mRNA expression is enhanced during HCC development in this model.

We further localized Pim-3 protein immunohistochemically in liver tissues obtained from HBsTg mouse after splenocyte transfer. We failed to detect Pim-3 protein in unmanipulated mice (Fig. 2A) or 9 month after splenocyte transfer, when hepatocytes with atypical nuclear configuration were not detected (data not shown). On the contrary, Pim-3 protein was weakly detected in the cytoplasm of hepatocytes with atypical nuclear configurations in pre-malignant lesion (Fig. 2B and E) and highly differentiated neoplastic hepatocytes in the tumor portion[7] (Fig. 2C and F). Moreover, Pim-3 protein was detected in regenerated proliferating bile ductules (Fig. 2D, arrow), which are assumed to be the proliferation of hepatic stem cells after the chronic liver injury such as infection and tumor[14]. These results may indicate that Pim-3 protein expression was aberrantly enhanced in liver during the course of hepatocarcinogenesis in this model.

Cloning and determination of nucleotide sequence of human Pim-3

Because the full length human Pim-3 cDNA nucleotide sequence has not been determined yet, we initially cloned and determined the nucleotide sequence of human Pim-3 cDNA by screening cDNA library constructed from a human hepatoma cell line, HepG2. Three positive clones were obtained after two rounds of screening, and these three distinct cDNA clones contained the same insertion, which consists of 2,392 bp. The 5'-untranslated region is 82.3 % G and C, while the 3'-untranslated region contains 5 copies of the ATTTA motif and 8 copies of TATT motif (Fig. 3A). This sequence exhibits an identity with a partial human Pim-3 cDNA sequence predicted from EST database (data not shown) [15]. Its open reading frame encodes the protein consisting of 326 amino acids with a calculated molecular weight of 35,861 (Fig. 3A). Moreover, the amino acid sequence of the predicted open reading frame, shares a high degree of identity with the mouse[16] and rat Pim-3 (KID-1) [8] proteins (95.0 %; Fig. 3B). Based on these results, we judged this clone as human Pim-3 cDNA. Human Pim-3 protein showed a high sequence identity with the quail qPim[17] (73.9 %) and *Xenopus* Pim (Pim-1) [18] (68.7 %) at the amino acid level (data not shown). Moreover, human Pim-3 protein shows a high sequence identity with human Pim-1[19] (57.1 %) and Pim-2[20] (44.0 %) at the amino acid level (Fig. 3C). Northern blotting analysis detected 2.4-kb mRNA in various organs including heart, skeletal muscle, brain, spleen, kidney, placenta, lung, and peripheral blood leukocytes (Fig. 4). In contrast, no specific band was detected in colon, thymus, liver, and small intestine under the present experimental conditions (Fig. 4).

Pim-3 is expressed aberrantly in human HCC

Immunohistochemical analysis failed to detect Pim-3 protein in normal liver tissues (Fig. 5A), consistent with the Northern blotting analysis. On the contrary, Pim-3 protein was weakly but diffusely detected in most of large regenerative nodules and adenomatous hyperplasia, lesions with precancerous potential, which were located adjacent to HCC areas (19 of 27 cases; Fig. 5B and 5C). Moreover, a substantial proportion of HCC cells were immunostained with anti-Pim-3 IgY (6 of 27

cases; Fig. 5D and 5E) but not the pre-immunized IgY (data not shown). Furthermore, Pim-3 protein was observed markedly in regenerated proliferating bile ductules (27 of 27 cases; Fig. 5C and 5F, arrows). Because the staining patterns were similar to that observed in HBsTg mouse model (see Fig 2), these results would indicate that Pim-3 protein expression was aberrantly enhanced in precancerous lesion, also in humans, and a portion of HCC cells.

Constitutive Pim-3 expression in human hepatoma cell lines

Immunohistochemical analysis indicated that Pim-3 protein expression was aberrantly enhanced not only in precancerous lesion but also in a portion of HCC cells in human HCC tissues (Fig. 5). This finding prompted us to examine Pim-3 expression in human hepatoma cell lines, by RT-PCR. To exclude the possibility that contaminated genomic DNA gave rise to the generation of the amplified bands, we used total RNA samples that were treated with DNase. Under the present condition, Pim-3 transcript was detected in all hepatoma cell lines, whereas no specific band was detected in the normal liver tissue (Fig. 6A), consistent with the Northern blotting analysis. The exclusion of reverse transcriptase failed to give rise to any bands, further indicating the specificities of RT-PCR (Fig. 6A non-RT). Moreover, an immunocytochemical analysis detected immunoreactive Pim-3 proteins in HuH7 cell line, when incubated with anti-Pim-3 antibodies (Fig. 6B-a) but neither pre-immunized IgY (Fig. 6B-b) nor anti-Pim-3 adsorbed with the relevant peptide (Fig. 6B-c). Immunoreactive Pim-3 proteins were similarly detected in all six human hepatoma cell lines, consistent with RT-PCR analysis (data not shown). Collectively, these results would indicate that Pim-3 was constitutively expressed in human hepatoma cell lines.

RNAi ablation of Pim-3 induces cell death to hepatoma cell lines

Because Pim-1 and Pim-2 were required to induce cell cycle progression[21, 22] and anti-apoptotic effects[21-25], we next examined the role of Pim-3 in cell proliferation, by ablating endogenous Pim-3 mRNA expression in HuH7 and Hep3B cell lines with RNAi. Endogenous Pim-3 mRNA level was decreased after the transfection with

specific Pim-3 siRNA but not Scramble siRNA (Fig. 7A). Under these conditions, transfection with Pim-3 siRNA significantly retarded cell proliferation, compared with Scramble siRNA-transfected and the control cells (Fig. 7B and C). These results suggested that Pim-3 ablation has adverse effects on the proliferation of hepatoma cell lines. We further observed that HuH7 cells detached from the plates later than 4 days after the transfection with Pim-3 but not Scramble siRNA (Fig. 8A). Moreover, Pim-3 siRNA transfectants exhibited a higher ratio of sub-G1 populations with reduced G1 and G2/M populations, compared with Scramble siRNA transfectants and control cells (Fig. 8B). Furthermore, the proportion of cells with condensed nuclei was significantly higher in both HuH7 and Hep3B cells transfected with Pim-3 siRNA, than those transfected with Scramble siRNA (Fig. 8C). These observations would indicate that the ablation of Pim-3 might induce apoptosis in these hepatoma cell lines.

DISCUSSION

Transcriptome analysis has been widely applied to elucidate molecular mechanisms of various types of diseases and can provide many important clues, particularly for understanding the molecular pathogenesis of oncogenesis, where the expression of many genes changes simultaneously[26, 27]. Several independent groups performed transcriptomal studies on human HCC[28-33]. However, in most studies, the gene expression pattern was compared between tumor and non-tumor portions obtained from the same patients[28-33]. Because these non-tumor portions exhibit usually hepatocyte dysplasia, this type of analysis may fail to detect the changes in gene expression that have already existed at the stage of hepatocyte dysplasia. In order to circumvent these pitfalls, we compared gene expression patterns between pre-malignant lesions and normal tissues by using FDD. We observed that various genes were selectively changed in pre-malignant lesions. Moreover, a semi-quantitative RT-PCR analysis did not detect any significant differences in the expression of several of these genes between malignant and pre-malignant lesions (our unpublished data), supporting our assumption that the changes in gene expression which have already existed at the stage of hepatocyte dysplasia, might be undetected in the preceding studies.

Among the genes identified in this study, we focused on Pim-3. Pim-3 was originally identified as depolarization-induced gene KID-1 in PC12 cell line, a rat pheochromocytoma cell line[8]. Subsequently, several independent groups observed a selective expression of its mRNA in neuronal system[16, 34, 35], but not liver. By using human Pim-3 cDNA as a probe, we detected Pim-3 mRNA in several organs such as brain and spleen, but not liver. On the contrary, Pim-3 mRNA expression was detected in all human hepatoma cell lines that we examined. Moreover, immunohistochemical analysis detected immunoreactive Pim-3 protein in precancerous lesions and a portion of HCC cells. Furthermore, Pim-3 protein was also detected in regenerating bile ductules, which are assumed to be the proliferation of hepatic stem cells after the

chronic liver injury such as infection and tumor[14]. Liver cell destruction and regeneration are thought to prepare the mitogenic, mutagenic environment, and impaired liver regeneration leading to HCC development[36]. Thus, Pim-3 expression may aberrantly be enhanced from hepatocyte regeneration process to its malignant transformation.

Deneen and colleagues provided evidence on the crucial involvement of Pim-3 in EWS/ETS-mediated malignant transformation of mouse NIH 3T3 cells[37]. They demonstrated that Pim-3 was a common transcriptional target of EWS/ETS. EWS/ETS fusion proteins retain an intact ETS DNA-binding domain and can bind to a binding sequence in the target genes through this domain[38]. Thus, Pim-3 gene transcription may be regulated not only by EWS/ETS fusion proteins but also other Ets family proteins. Several independent groups reported that Ets-1, one of the Ets family proteins, was expressed in human HCC tissues[39, 40]. Ito and colleagues described that Ets-1 expression was markedly enhanced in non-cancerous lesions adjacent to HCC lesions and suggested that Ets-1 had a crucial role in hepatocarcinogenesis and HCC progression during their early phases[39]. In line with these observations, we also observed that another transcription factor with an ETS-domain, polyomavirus enhancer A binding protein-3, was expressed selectively in HCC and that polyomavirus enhancer A binding protein-3 induced constitutive gene expression of a pro-angiogenic factor, interleukin (IL)-8, in HCC[41]. Thus, it is tempting to speculate that a transcription factor(s) with an ETS-domain, may induce ectopic Pim-3 gene expression in liver, during the course of hepatocarcinogenesis.

Several lines of evidence demonstrated that the gene expression of Pim-1 and Pim-2 could be regulated by IL-6-gp130-mediated signal transducers and activators of transcription (STAT) family protein, STAT3[42, 43]. STAT3 signals can advance cell cycles and prevent apoptosis by inducing Pim-1 and c-Myc in lymphomagenesis[43]. In the liver, IL-6-deficient mice exhibited an impaired liver regeneration after a partial hepatectomy[44]. Several lines of evidence have revealed that Bcl-xL expression is

up-regulated by IL-6-gp130-mediated STAT3 and prevents hepatocyte apoptosis[45, 46], and that the constitutive activation of STATs observed during oncogenesis can cause a permanent alteration in the genetic program[46, 47]. These observations suggest that STAT3 signals could regulate hepatocyte regeneration also during the course of HBV-induced hepatocarcinogenesis. We observed that Pim-3 gene ablation by RNAi attenuated proliferation rates and caused cell death in hepatoma cell lines. Thus, if Pim-3 was also regulated by STAT3, these observations suggest that Pim-3 would also be involved in STAT3-mediated prevention of apoptosis and/or cell cycle progression.

Pim-1 and Pim-2 are also known as proto-oncogene to be involved in lymphomagenesis[48, 49]. Because Pim-1 and Pim-2 can induce anti-apoptotic effects[21-25], Pim-3 may be involved in cell cycle regulation and/or anti-apoptosis. We also observed that gene ablation of Pim-3 caused cell death to human hepatoma cell lines, later than 3 days after the transfection. These results suggest that Pim-3 can regulate cell cycle and/or apoptosis process indirectly by phosphorylating a molecule(s) upstream in these processes. Although Pim-1 can phosphorylate several molecules such as Cdc25A[50], a G_1/S cell cycle regulator, Pim-3 could not interact with Cdc25A[37]. Pim-1 can also phosphorylate valosine containing protein (VCP)/p97[42, 43], a mammalian homolog of *Saccaromyces cerevisiae* Cdc48p. Pim-1 can up-regulate further the expression of an anti-apoptotic molecule, Bcl-2 and Bcl-xL, by augmenting the expression of VCP[42, 43]. In HCC tissues and human hepatoma cell lines, evidence is accumulating to indicate that Bcl-xL is constitutively expressed and is a major executer to prevent apoptosis[51-53]. Moreover, VCP was also detected in human HCC tissues[54]. If VCP could be phosphorylated by Pim-3 as well as Pim-1, Pim-3 may exert an anti-apoptosis effect by augmenting indirectly the expression of an anti-apoptotic molecule, similarly as Pim-1. Moreover, if the contents of target molecules may differ between HuH7 and Hep3B cell lines, these may account for different patterns of the effects of Pim-3 gene ablation on the proliferation of these cell lines.

The kinase activity of Pim-3 was crucially involved in EWS/ETS-mediated

malignant transformation of mouse NIH 3T3 cells[37]. Our present observations suggest that Pim-3 can regulate anti-apoptosis process and/or cell cycle progression probably by modulating molecules involved in these processes. Accumulating evidence indicated that Pim-3 can auto-phosphorylate itself[8, 17], but it still remains elusive on physiological substrates of Pim-3. The identification of a substrate(s) may shed novel light on Pim-3-mediated regulatory mechanisms of apoptosis and/or cell cycle progression.

REFERENCES

1. Schafer DF, Sorrell MF. Hepatocellular carcinoma. Lancet 1999; 353:1253-7.
2. Geller SA. Hepatitis B and hepatitis C. Clin Liver Dis 2002; 6:317-34.
3. Iino S. Natural history of hepatitis B and C virus infections. Oncology 2002; 62:18-23.
4. Bertoletti A, Maini MK. Protection or damage: a dual role for the virus-specific cytotoxic T lymphocyte response in hepatitis B and C infection? Curr Opin Immunol 2000; 12:403-8.
5. Hino O, Kajino K, Umeda T, Arakawa Y. Understanding the hypercarcinogenic state in chronic hepatitis: a clue to the prevention of human hepatocellular carcinoma. J Gastroenterol 2002; 37:883-7.
6. Nakamoto Y, Guidotti LG, Kuhlen CV, Fowler P, Chisari FV. Immune pathogenesis of hepatocellular carcinoma. J Exp Med 1998; 188:341-50.
7. Nakamoto Y, Suda T, Momoi T, Kaneko S. Different procarcinogenic potentials of lymphocyte subsets in a transgenic mouse model of chronic hepatitis B. Cancer Res. 2004; 64:3326-33.
8. Feldman JD, Vician L, Crispino M, Tocco G, Marcheselli VL, Bazan NG, Baudry M, and Herschman HR. KID-1, a protein kinase induced by depolarization in brain. J Biol Chem 1998; 273:16535-43.
9. Chisari FV, Filippi P, McLachlan A, Milich DR, Riggs M, Lee S, Palmiter RD, Pinkert CA, Brinster RL. Expression of hepatitis B virus large envelope polypeptide inhibits hepatitis B surface antigen secretion in transgenic mice. J Virol 1986; 60:880-7.
10. Wirth S, Guidotti LG, Ando K, Schlicht HJ, Chisari FV. Breaking tolerance leads to autoantibody production but not autoimmune liver disease in hepatitis B virus envelope transgenic mice. J Immunol 1995; 154:2504-15.
11. Ito T, Sakaki Y. Fluorescent differential display: a fast and reliable method for

message display polymerase chain reaction. Methods Enzymol 1999; 303:298-309.

12. Lu P, Nakamoto Y, Nemoto-Sasaki Y, Fujii C, Wang H, Hashii M, Ohmoto Y, Kaneko S, Kobayashi K, Mukaida N. Potential interaction between CCR1 and its ligand, CCL3, induced by endogenously produced interleukin-1 in human hepatomas. Am J Pathol 2003; 162:1249-58.
13. Kitamura K, Nakamoto Y, Akiyama M, Fujii C, Kondo T, Kobayashi K, Kaneko S, Mukaida N. Pathogenic roles of tumor necrosis factor receptor p55-mediated signals in dimethylnitrosamine-induced murine liver fibrosis. Lab Invest 2002; 82:571-83.
14. Wang X, Foster M, Al-Dhalimy M, Lagasse E, Finegold M, Grompe M. The origin and repopulating capacity of murine oval cells. Proc Natl Acd Sci USA 2003; 100:11881-8.
15. Mikkers H, Allen J, Knipscheer P, Romeyn L, Hart A, Vink E, Berns A. High-throughput retroviral tagging to identify components of specific signaling pathways in cancer. Nat Genet 2002; 32:153-9.
16. Konietzko U, Kauselmann G, Scafidi U, Staubli U, Mikkers H, Berns A, Schweizer M, Waltereit R, Kuhl D. Pim kinase expression is induced by LTP stimulation and required for the consolidation of enduring LTP. EMBO J 1999; 18:3359-69.
17. Eichmann A, Yuan L, Bréant C, Alitalo K, Koskinen PJ. Developmental expression of Pim kinases suggests functions also outside of the hematopoietic system. Oncogene 2000; 19:1215-24.
18. Palaty CK, Kalmar G, Tai G, Oh S, Amankawa L, Affolter M, Aebersold R, Pelech SL. Identification of the autophosphorylation sites of the *Xenopus laevis* Pim-1 proto-oncogene-encoded protein kinase. J Biol Chem 1997; 272:10514-21.
19. Houri RZ, Hazum S, Givol D, Telerman A. The cDNA sequence and gene analysis of the human *pim* oncogene. Gene 1987; 54:105-11.
20. Baytel D, Shalom S, Madger I, Weissenberg R, Don J. The human *Pim-2* proto-oncogene and its testicular expression. Biochim Biophis Acta 1998;

1442:274-85.

21. Möröy T, Grzeschiczek A, Petzold S, Hartmann KU. Expression of a *Pim-1* transgene accelerates lymphoproliferation and inhibits apoptosis in *lpr/lpr* mice. Proc Natl Acd Sci USA 1993; 90:10734-8.
22. Wang Z, Bhattacharya N, Weaver M, Petersen K, Meyer M, Gapter L, Magnuson NS. Pim-1: a serine/threonine kinase with a role in cell survival, proliferation, differentiation and tumorigenesis. J Vet Sci 2001; 2:167-79.
23. Skorska MN, Hoser G, Kossev P, Wasik MA, Skorski T. Complementary functions of the antiapoptotic protein A1 and serine/threonine kinase pim-1 in the BCR/ABL-mediated leukemogenesis. Blood 2002; 99:4531-9.
24. Fox CJ, Hammerman PS, Cinalli RM, Master SR, Chodosh LA, Thompson CB. The serine/threonine kinase Pim-2 is a transcriptionally regulated apoptotic inhibitor. Genes Dev 2003; 17:1841-54.
25. Yan B, Zemskova M, Holder S, Chin V, Kraft A, Koskinen PJ, Lilly M. The PIM-2 kinase phosphorylates BAD on serine 112 and reverses BAD-induced cell death. J Biol Chem 2003; 278:45358-67.
26. Liotta L, Petricoin E. Molecular profiling of human cancer. Nature Rev Genet 2000; 1:48-56.
27. Thorgeirsson SS, Grisham JW. Molecular pathogenesis of human hepatocellular carcinoma. Nat Genet 2002; 31:339-46.
28. Honda M, Kaneko S, Kawai H, Shirota Y, Kobayashi K. Differential gene expression between chronic hepatitis B and C hepatic lesion. Gastroenterology 2001; 120:955-66.
29. Kim MY, Park E, Park JH, Park DH, Moon WS, Cho BH, Shin HS, Kim DG. Expression profile of nine novel genes differentially expressed in hepatitis B virus-associated hepatocellular carcinomas. Oncogene 2001; 20:4568-75.
30. Shirota Y, Kaneko S, Honda M, Kawai HF, Kobayashi K. Identification of differentially expressed genes in hepatocellular carcinoma with cDNA microarrays.

Hepatology 2001; 33:832-40.

31. Smith MW, Yue ZN, Geiss GK, Sadovnikova NY, Carter VS, Boix L, Lazaro CA, Rosenberg GB, Bumgarner RE, Fausto N, Bruix J, Katze MG. Identification of novel tumor markers in hepatitis C virus-associated hepatocellular carcinoma. Cancer Res 2003; 63:859-64.
32. Xu XR, Huang J, Xu ZG, Qian BZ, Zhu ZD, Yan Q, Cai T, Zhang X, Xiao HS, Qu J, Liu F, Huang QH, Cheng ZH, Li NG, Du JJ, Hu W, Shen KT, Lu G, Fu G, Zhong M, Xu SH, Gu WY, Huang W, Zhao XT, Hu GX, Gu JR, Chen Z, Han ZG. Insight into hepatocellular carcinogenesis at transcriptome level by comparing gene expression profiles of hepatocellular carcinoma with those of corresponding noncancerous liver. Proc Natl Acd Sci USA 2001; 98:15089-94.
33. Yamashita T, Kaneko S, Hashimoto S, Sato T, Nagai S, Toyoda N, Suzuki T, Kobayashi K, Matsushima K. Serial analysis of gene expression in chronic hepatitis C and hepatocellular carcinoma. Biochem Biophys Res Commun 2001; 282:647-54.
34. Giza CC, Prins ML, Hovda DA, Herschman HR, Feldman JD. Genes preferentially induced by depolarization after concussive brain injury: Effects of age and injury severity. J Neurotrauma 2002; 19:387-402.
35. Lu A, Tang Y, Ran R, Clark JF, Aronow BJ, Sharp FR. Genomics of the periinfarction cortex after focal cerebral ischemia. J Cereb Blood Flow Metab 2003; 23:786-810.
36. Michalopoulos GK, DeFrances MC. Liver regeneration. Science 1997; 276:60-6.
37. Deneen B, Welford SM, Ho T, Hernandez F, Kurland I, Denny CT. PIM3 proto-oncogene kinase is a common transcriptional target of divergent EWS/ETS oncoproteins. Mol Cell Biol 2003; 23:3897-908.
38. Arvand A, Denny CT. Biology of EWS/ETS fusions in Ewing's family tumors. Oncogene 2001; 20:5747-54.
39. Ito Y, Miyoshi E, Takeda T, Sakon M, Noda K, Tsujimoto M, Monden M, Taniguchi

N, Matsuura N. Expression and possible role of *ets-1* in hepatocellular carcinoma. Am J Clin Pathol 2000; 114:719-25.

40. Kanda K, Nakayama T, Onizuka S, Tomioka T, Kanematsu T. Expression of the Ets-1 proto-oncogene is linked to cell differentiation of human hepatocellular carcinoma. Hepatogastroenterology 2002; 49:746-51.
41. Iguchi A, Kitajima I, Yamakuchi M, Ueno S, Aikou T, Kubo T, Matsushima K, Mukaida N, Maruyama I. PEA3 and AP-1 are required for constitutive IL-8 gene expression in hepatoma cells. Biochem Biophys Res Commun 2000; 279:166-71.
42. Hirano T, Ishihara K, Hibi M. Roles of STAT3 in mediating the cell growth, differentiation and survival signals relayed through the IL-6 family of cytokine receptors. Oncogene 2000; 19:2548-56.
43. Shirogane T, Fukada T, Muller JMM, Shima DT, Hibi M, Hirano T. Synergistic roles for Pim-1 and c-Myc in STAT3-mediated cell cycle progression and antiapoptosis. Immunity 1999; 11:709-19.
44. Cressman DE, Greenbaum LE, DeAngelis RA, Ciliberto G, Furth EE, Poli V, Taub R. Liver failure and defective hepatocyte regeneration in interleukin-6-deficient mice. Science 1996; 274:1379-83.
45. Wuestefeld T, Klein C, Streetz KL, Betz U, Lauber J, Buer J, Manns MP, Müller W, Trautwein C. Interleukin-6/glycoprotein 130-dependent pathways are protective during liver regeneration. J Biol Chem 2003; 278:11281-8.
46. Bowman T, Garcia R, Turkson J, Jove R. STATs in oncogenesis. Oncogene 2000; 19:2474-88.
47. Bromberg J. Stat proteins and oncogenesis. J Clin Invest 2002; 109:1139-42.
48. van Lohuizen M, Verbeek S, Krimpenfort P, Domen J, Saris C, Radaszkiewicz T, Berns A. Predisposition to lymphomagenesis in *pim-1* transgenic mice: cooperation with *c-myc* and *N-myc* in murine leukemia virus-induced tumors. Cell 1989; 56:673-82.
49. Allen JD, Verhoeven E, Domen J, van der Valk M, Berns A. *Pim-2* transgene

induces lymphoid tumors, exhibiting potent synergy with *c-myc*. Oncogene 1997; 15:1133-41.

50. Takehara T, Liu X, Fujimoto J, Friedman SL, Takahashi H. Expression and role of Bcl-xL in human hepatocellular carcinomas. Hepatology 2001; 34:55-61.
51. Mochizuki T, Kitanaka C, Noguchi K, Muramatsu T, Asai A, Kuchino Y. Physical and functional interactions between Pim-1 kinase and Cdc25A phosphatase. J Biol Chem 1999; 274:18659-66.
52. Pierce RH, Vail ME, Ralph L, Campbell JS, Fausto N. Bcl-2 expression inhibits liver carcinogenesis and delays the development of proliferating foci. Am J Pathol 2002; 160:1555-60.
53. Watanabe J, Kushihata F, Honda K, Mominoki K, Matsuda S, Kobayashi N. Bcl-xL overexpression in human hepatocellular carcinoma. Int J Oncol 2002; 21:515-19.
54. Yamamoto S, Tomita Y, Nakamori S, Hoshida Y, Nagano H, Dono K, Umeshita K, Sakon M, Monden M, Aozasa K. Elevated expression of valosin-containing protein (p97) in hepatocellular carcinoma is correlated with increased incidence of tumor recurrence. J Clin Oncol 2003; 21:447-52.

TABLE 1.

Identification of genes differentially expressed in pre-malignant lesion of HBsTg mice

classification	description	accession number
up-regulated		
transcription factors	Y box protein 3	AK029441
immune system proteins	complement component 3	BC043338
xenobiotic metabolism	ceruloplasmin	NM_00775
	metallothionein II	AK002567
oncogenes	24p3 (lipocalin 2)	X81627
metabolism enzymes	aldehyde dehydrogenase family 1, subfamily A1	BC044729
	hemoglobin α, adult chain 1	NM_008218
	phosphoenolpyruvate carboxy-kinase 1	NM_011044
	succinate dehydrogenase complex, subunit A flavoprotein	BC031849
growth factors, cytokines, and chemokines	growth differentiation factor 15 (macrophage inhibiting compound-1)	NM_011819
	insulin-like growth factor binding protein 1	NM_008341
non-receptor protein kinases	serine/threonine kinase pim-3	NM_145478
not classified	betaKlotho	AF178429
	pol protein	XM_196572
	serine (or cysteine) proteinase inhibitor, clade A, member 6	NM_007618
putative proteins	hypothetical Esterase/acetylhydrolase structure containing protein	NM_026347
	putative e1 protein	AK090127
	similar to bile acid Coenzyme A: amino acid N-acyltransferase	NM_145368
est		AW047153
		BE132832
		BB168703
		BM224373
unknown	fibronectin non-coding region	
	hypothetical protein non-coding region chromosome 5	
down-regulated		
immune system proteins	β2-microglobulin	□□□□□□
	complement component C1SA	AF459017
extracellular transport/carrier proteins	serum amyloid A-1	M13521
metabolism enzymes	cytochrome P450 4A10	BC031141
	hemoglobin β, adult major chain	AK027904
	stearoyl-Coenzyme A desaturase 1	BC007474
	isocitrate dehydrogenase 1 (NADP+), soluble	AK087063
not classified	endogenous retrovirus 3' LTR	K02892
	glutatione S-transferase	BC009805
	group1 major urinary protein	X03208
	major urinary protein 1	BC012221
	major urinary protein 2	BC012259

	major urinary protein 3	XM_135398
	major urinary protein 11 and 8	AK011413
	preimplantation protein 2	AK028563
	ubiquitin-associated protein 1	NM_023305
mitchondrial gene	cytochrome oxidase A1	V00711
putative proteins	archerase	AY071852
	dis3 protein homolog	AK032091

FIGURE LEGENDS

FIGURE 1. Semi-quantitative RT-PCR analysis for proto-oncogene *Pim* family mRNA expression in HBsTg mice.

A. Total RNAs were extracted from HBsTg mice before (symbol N), 9 (whole liver, symbol 9), 15 months (pre-malignant lesions, symbol 15) after splenocyte transfer, or transgenic splenocytes transfer (symbol C).

B. Total RNAs were extracted from pre-malignant (symbol P) or malignant (symbol M) tissues of HBV transgenic mice 15 months after splenocyte transfer.

Representative results from three independent experiments are shown in the upper panels. The ratios of the PCR product for Pim-3 to GAPDH were determined, and relative intensities were calculated to assume the ratio of untreated mice as 1.0. Then, means and SD were calculated and are shown in the lower panels. Statistical significance was evaluated using ANOVA test, and $p < 0.05$ was accepted as statistically significant. *, $p < 0.05$ compared with N.

FIGURE 2. Immunohistochemical analysis of Pim-3 in HBsTg mice. HBsTg mice liver tissues before (A) and 15 months after splenocyte transfer (B, D, and E, non-tumor portions; C and F, tumor potions) were immunostained by anti-Pim-3 IgY as described in Materials and Methods. Representative results are shown here.

B. Pre-malignant lesion is indicated with arrowheads.

C. Tumor portion is indicated with arrowheads.

D. The positively stained regenerated proliferating bile ductule. The arrow indicates regenerated proliferating bile ductule.

E and F. The positively stained hepatocytes at a higher magnification of the square in B and C.

Original magnification; A to C, x 100; D to F, x 400. Scale bars are 50 μm.

FIGURE 3. A. Structure of human Pim-3 cDNA. The nucleotide and predicted amino acid sequences of human Pim-3 are shown. The nucleotide sequence is numbered. The predicted amino acid sequence is shown in a single-letter code below the nucleotide sequence. The AT-rich motifs are indicated in boxes and highlights. The region used as the probe for Northern blot analysis is underlined.

B. and C. Amino acid alignment of *Pim* family proteins. The amino acid sequences of human, rat, and mouse Pim-3s (B) or other members of human *Pim* family kinases (C) were aligned using DNASIS-Mac version 3.0 software (Hitachi Software Engineering Co., Ltd., Yokohama, Japan). The residues identical to human Pim-3 are highlighted.

FIGURE 4. Human Pim-3 mRNA expression in human normal tissues. Northern blot analysis was performed as described in Materials and Methods, and representative results are shown here. sk. muscle, skeletal muscle; PBL, peripheral blood leukocytes. GAPDH mRNA expression was analyzed in parallel to evaluate the amount of mRNA loaded in each lane.

FIGURE 5. Immunohistochemical analysis of Pim-3 in HCC tissues. Human normal liver tissue (A) or HCC tissues (B to F) were immunostained by anti-Pim-3 IgY as described in Materials and Methods. Representative results are shown here.

B. Precancerous lesions. The lesions surrounded with arrowheads and arrows are precancerous lesions and HCC lesions, respectively.

C. Precancerous lesion in the square of B is shown at a higher magnification. Arrows indicate regenerated proliferating bile ductules.

D and E. The positively stained HCC cells. E indicates the square in D at a higher magnification.

F. The positively stained regenerated proliferating bile ductules at a higher magnification of the square in D. Arrows indicate regenerated proliferating bile

ductules.

Original magnification; A, B and D, x 100; C, E, and F, x 400. Scale bars are 50 μm.

FIGURE 6. A. Pim-3 mRNA expression in various human hepatoma cell lines. Total RNAs were extracted from human hepatoma cell lines and normal liver tissue. RT-PCR was performed, and representative results from three independent experiments are shown here. Analysis for Pim-3 expression was performed without reverse transcriptase treatment and the results are shown as non-RT.

B. Pim-3 protein expression in HuH7 cells. HuH7 cells were immunostained by anti-Pim-3 IgY (B-a), by pre-immunized IgY (B-b), or by anti-Pim-3 antibodies absorbed with the relevant peptide (B-c) as described in Materials and Methods. Representative results from three independent experiments are shown here. Original magnification, x 400. Scale bars are 50 μm.

FIGURE 7. The effects of endogenous Pim-3 ablation on cell proliferation.

A. Semi-quantitative RT-PCR analysis for Pim-3 mRNA levels in siRNA transfected cells. Total RNAs were extracted from the transfectant with Pim-3 siRNA (symbol P), Scramble siRNA (symbol S), or no siRNA (symbol N) 2 (Hep3B) or 4 days (HuH7) after the transfection as described in Materials and Methods.

B and C. Cell proliferation rates were determined on HuH7 (B) and Hep3B (C) cells transfected with Pim-3 siRNA (circles), Scramble siRNA (squares), or no siRNA (triangles) by WST-1 assay. Cells were trypsinized and 5 x 10^3 cells were plated to each well of 96-well plate at 2 days after the transfection. This time point was designated as day 0. The ratios to day 0 were calculated. Results are expressed as means (n = 3), and error bars indicate SD. Representative results from three independent experiments are shown here. Statistical significance was evaluated using ANOVA test, and $p< 0.05$ was accepted as statistically significant. *, $p < 0.05$ compared with no siRNA samples at the same time point.

FIGURE 8. The effects of endogenous Pim-3 ablation on apoptosis in HuH7 cells.

A. HuH7 cells were observed under an inverted microscope at 4 days after the transfection with Pim-3 or Scramble siRNA under the same conditions as FIG. 7. Representative results from three independent experiments are shown here. Original magnification, x 200. Scale bars are 50 μm.

B. Cell cycles were analyzed at 4 days after the transfection, by using a flow cytometry as described in Materials and Methods. Representative results from three independent experiments are shown here.

C. Chromatin condensation was analyzed at 4 days after the transfection as described in Materials and Methods. Representative results from three independent experiments are shown here. Results are expressed as means (n = 6), and bars indicate SE. Statistical significance was evaluated using ANOVA test, and $p < 0.05$ was accepted as statistically significant. *, $p < 0.05$ compared with Scramble siRNA samples.

Figure 1, Fujii *et al.*

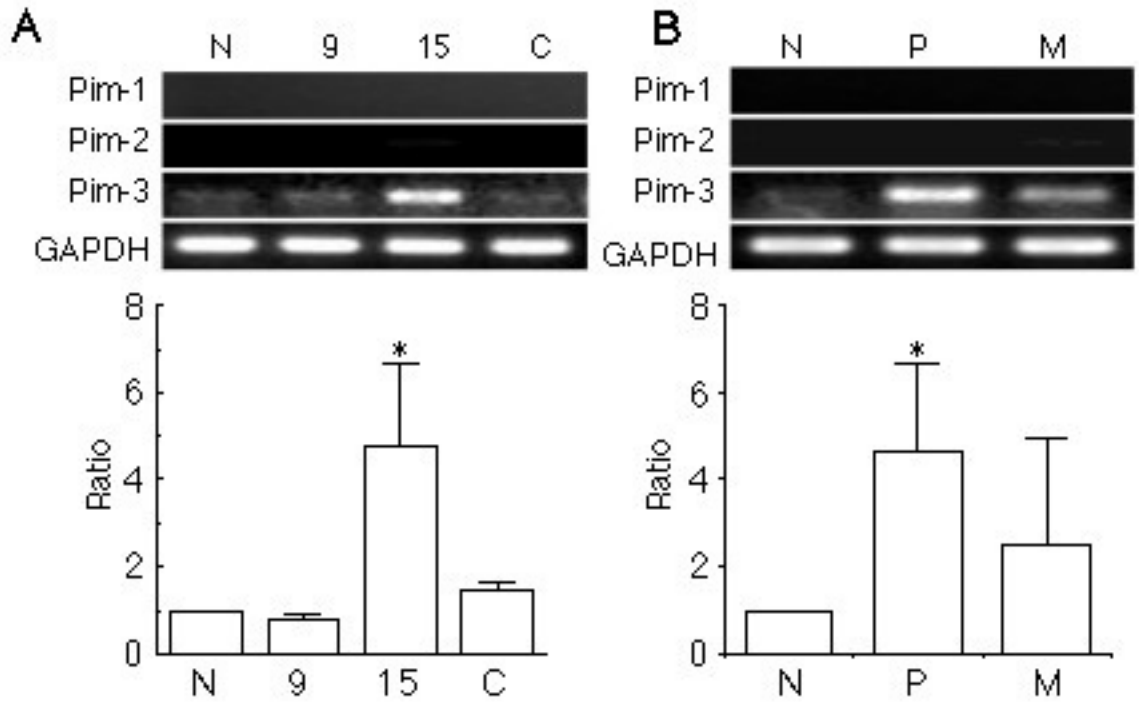

Figure 2, Fujii *et al.*

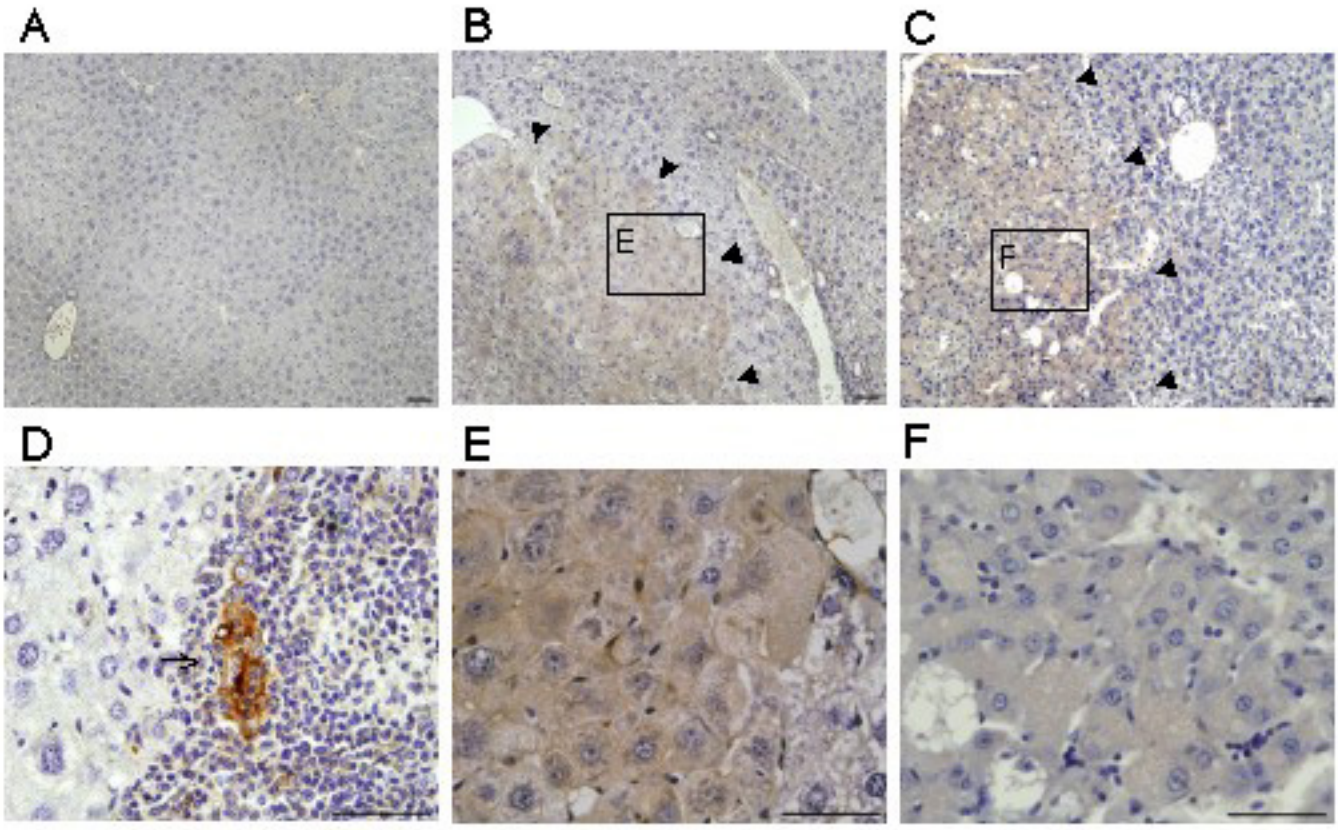

Figure 3, Fujii *et al.*

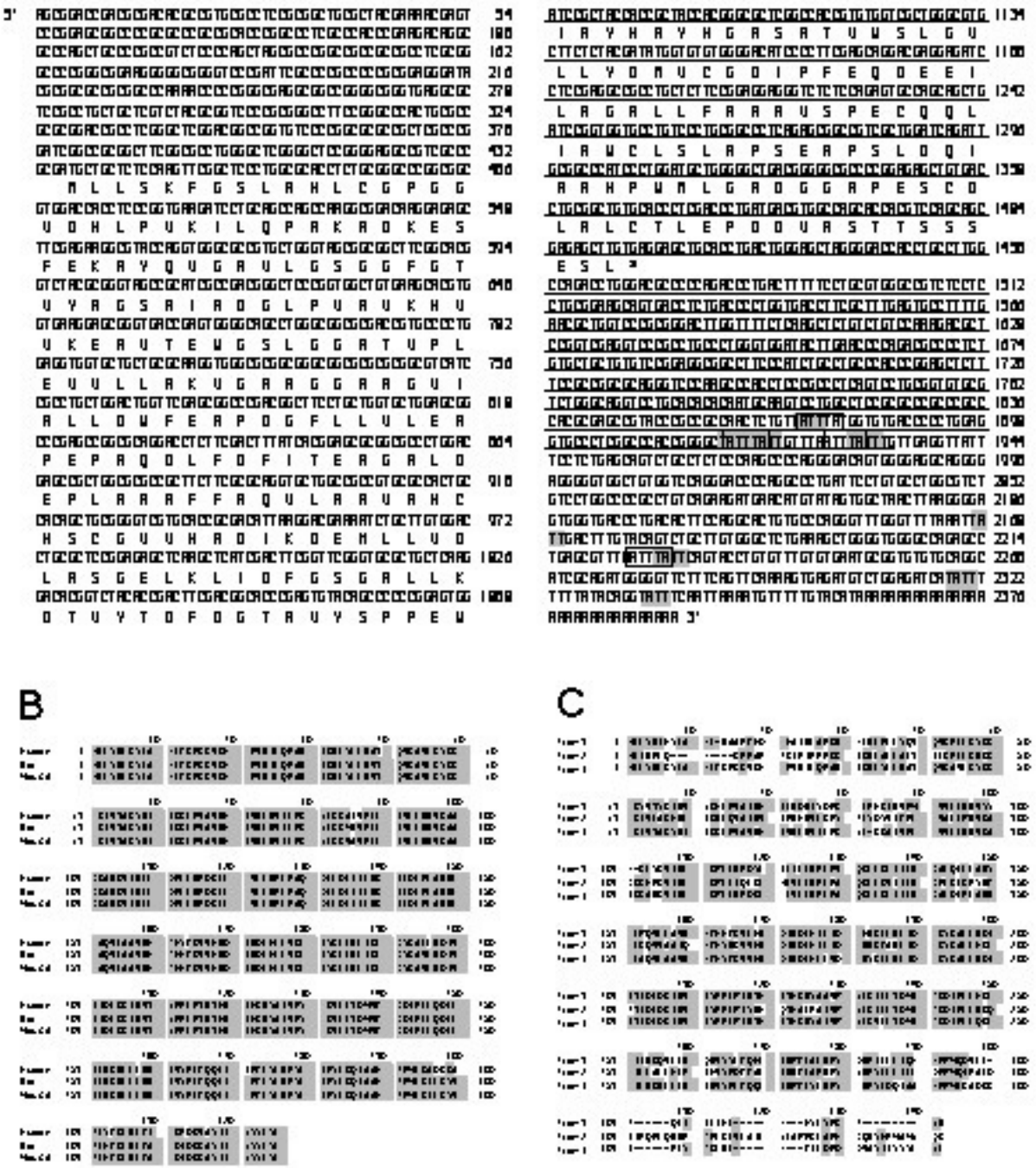

Figure 4, Fujii *et al.*

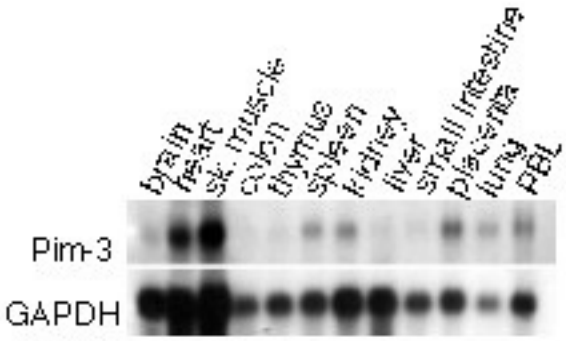

Figure 5, Fujii *et al.*

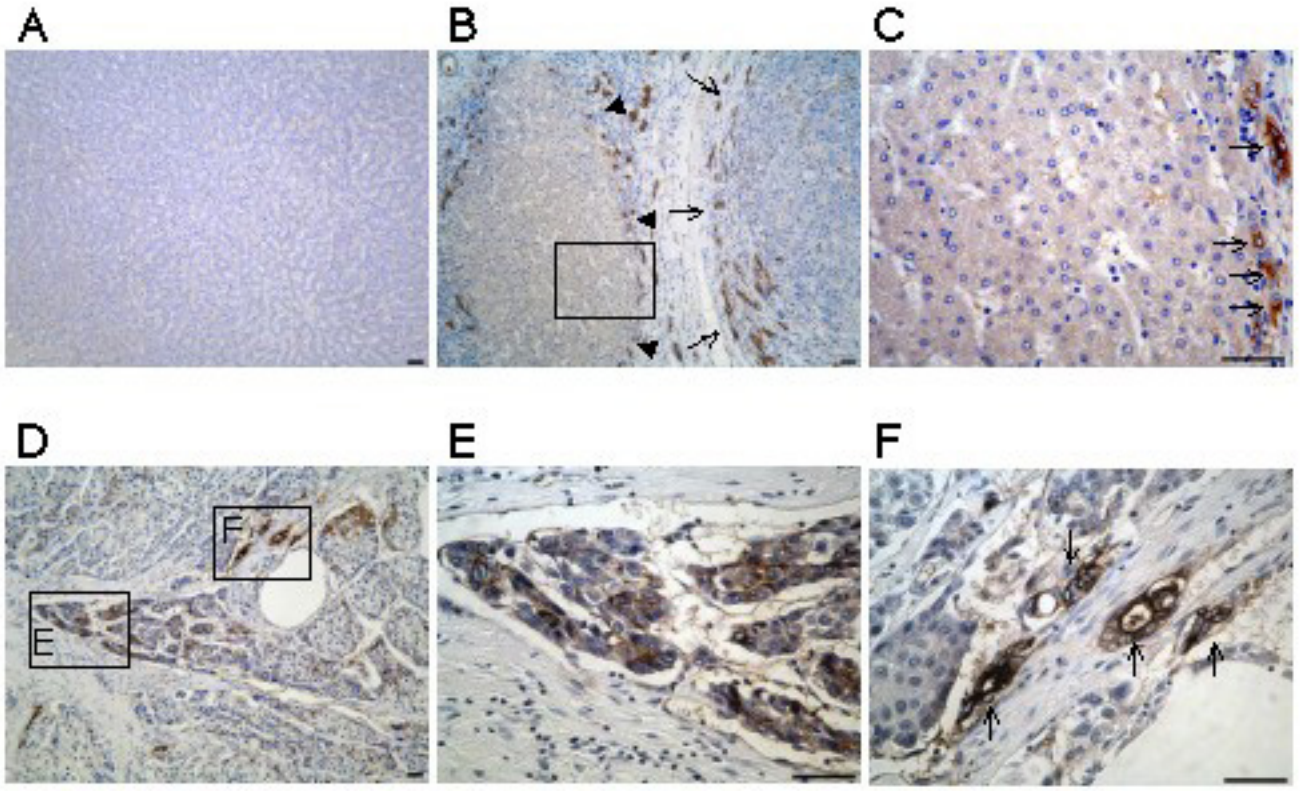

Figure 6, Fujii *et al.*

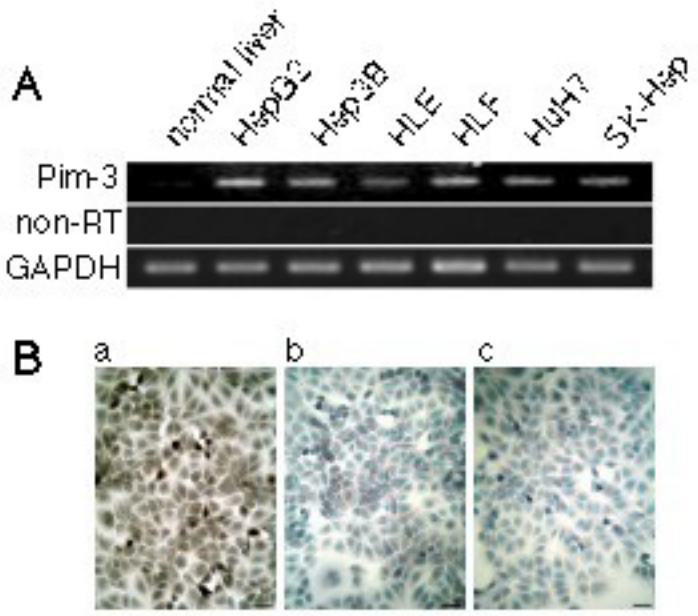

Figure 7, Fujii *et al.*

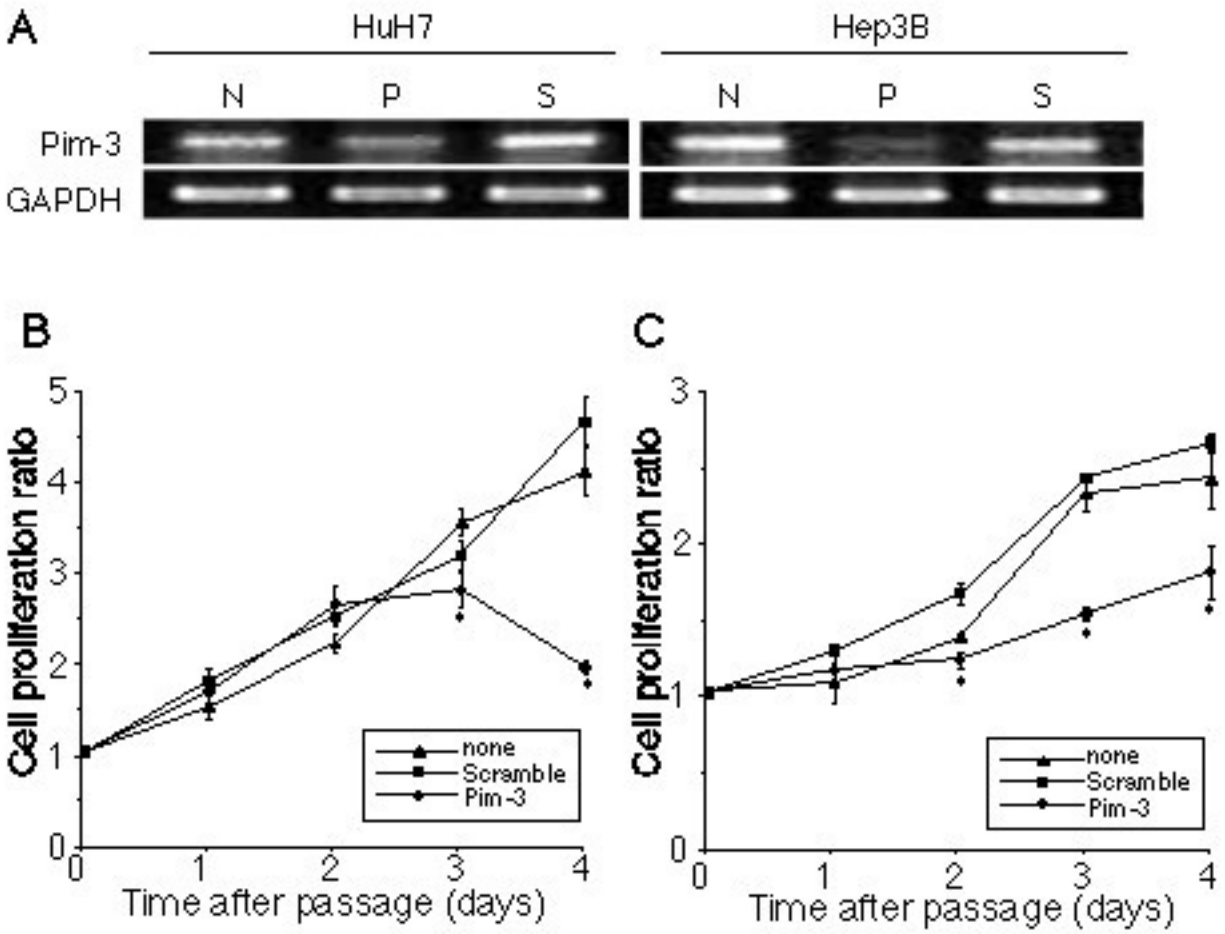

Figure 8, Fujii *et al.*